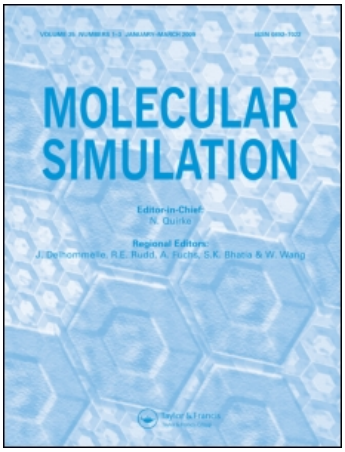

Molecular Simulation
Publication details, including instructions for authors and subscription information:
http://www.informaworld.com/smpp/title~content=t713644482

The relationship between structure and electrochemical property of cyanoimino derivatives of squaric acid

Z. -M. Xue[a]; C. -H. Chen[b]
[a] Department of Chemistry, Anhui University, Anhui, Hefei, P.R. China [b] Department of Materials Science and Engineering, University of Science and Technology of China, Anhui, Hefei, P.R. China

To cite this Article Xue, Z. -M. and Chen, C. -H.(2006) 'The relationship between structure and electrochemical property of cyanoimino derivatives of squaric acid', Molecular Simulation, 32: 5, 401 — 408
To link to this Article: DOI: 10.1080/08927020600669999
URL: http://dx.doi.org/10.1080/08927020600669999

Molecular Simulation, Vol. 32, No. 5, 30 April 2006, 401–408

Taylor & Francis
Taylor & Francis Group

The relationship between structure and electrochemical property of cyanoimino derivatives of squaric acid

Z.-M. XUE†‡* and C.-H. CHEN†

†Department of Materials Science and Engineering, University of Science and Technology of China, Hefei, Anhui 230026, P.R. China
‡Department of Chemistry, Anhui University, Hefei, Anhui 230039, P.R. China

(Received December 2005; in final form March 2006)

Theoretical studies on anions of 1,2-dihydroxycyclobuten-3,4-dione (squaric acid, H_2SQ) and the whole series of cyanoimino derivatives in gas-phase and in acetonitrile (AN) solution are carried out using density functional theory (DFT) and SCRF-DFT method at B3LYP theory level for the first time. Natural bond orbital (NBO) analyses indicate that π-electron delocalization in the series is quite strong. The GIAO-DFT results for all dianions suggest that the corresponding B3LYP/6-31 + G(d,p) geometries can be deemed reasonably good representations of the geometries of the relatively free dianions in solution. Based on the most stable conformations, linear correlations are observed between the oxidation potential measured by cyclic voltammetry and the highest occupied molecular orbital (HOMO) energy as well as ionization potential (I_p), which support experimental results that systematic substitution of the oxygen atoms in the $C_4O_4^{2-}$ structure with NCN groups causes a shift of both the oxidation potentials $\mathbf{E}_1^0$ and $\mathbf{E}_2^0$ towards more positive values. The correlations are also observed between experimental K_{sem} and Gibbs free energy calculated in AN solution.

Keywords: Cyanoimino derivatives; Squaric acid; Gibbs free energy; Density functional theory

1. Introduction

1,2-Dihydroxycyclobuten-3,4-dione (squaric acid, H_2SQ, 1) and the whole series of dicyanomethylene derivatives have been synthesized [1] and studied experimentally in some detail because they could accomplish, in principle, many of the requirements which are recognized to favor the display of unusual, at least for organic materials, electric, magnetic and optical properties in the solid state [2–8]. Compared with them, the whole series of cyanoimino derivatives (Scheme 1) have also been synthesized but not studied experimentally in as detail as the formers [9]. Since comprehensive investigation of the physicochemical properties is an essential step for the evaluation of the potential utility of these compounds, the results of a detailed electrochemical study have been reported on the whole series of cyanoimino derivatives of 1,2-dihydroxy-cyclobuten-3,4-dione [10].

Because the structure of anions (or radicals) plays an important role in determining to ionic conductivity, electrochemical windows [11–13], a thorough computational investigation on the electronic structures, energies and orbitals of the anions would be desirable to better our understanding their properties at a quantum chemistry level.

In this study, the density functional theory (DFT) B3LYP method [14,15] is chosen because it accounts better for electron correlation energies and greatly reduces the calculation expenses with rather reliable description of both geometries and energy of targeted molecules. We will address the following issues regarding the dianions: (a) the conformational characteristics of the anions; and (b) the relationship between anion structures and electrochemical properties [16].

2. Calculation method

The local minima of the di-, mono-anions and neutral products have been fully optimized by analytic gradient techniques. The method used is the DFT with Becke's three parameters (B3) exchange functional along with the Lee–Yang–Parr (LYP) non-local correlation functional (B3LYP). All of them are treated with DFT method at 6-31 + G(d,p) level for full geometry optimization. Natural population analysis (NPA) and natural bond orbital (NBO) [17] analysis are performed at the same level using NBO program to

*Corresponding author. Fax: 86 551 5106000. Email: zmxue@ahu.edu.cn.

Molecular Simulation
ISSN 0892-7022 print/ISSN 1029-0435 online © 2006 Taylor & Francis
http://www.tandf.co.uk/journals
DOI: 10.1080/08927020600669999

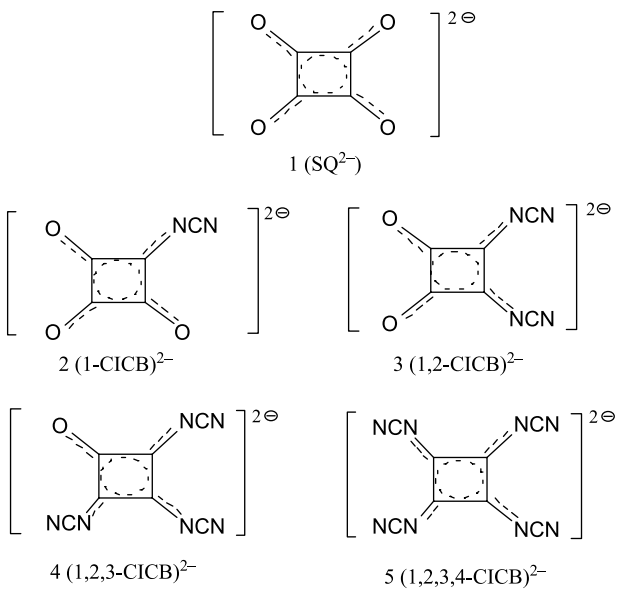

Scheme 1. The dianion structures of squaric acid and its cyanoimino derivatives.

obtain quantitative analysis of electronic structures. For the solvent calculations, the SCRF-PCM is used.

Single-point energy calculations at higher level basis set (B3LYP/6-31++G(3df,3pd)//B3LYP/6-31 + G(d,p)) are also performed to obtain more accurate energies. The HF method at the same level computation is performed for comparing with DFT at some cases. All of the HF, DFT, SCRF-PCM and NBO calculations are performed using the Gaussian 03 program package [18].

3. Results and discussion

3.1 Geometries

First, we shall present and discuss the results obtained for the "model" system di-, mono-anions and neutral product of **4**. The other four systems studied here will be discussed with reference to this system.

Table 1. Optimized geometries of the anions of group **4** *†.

	1,2,3-CICB	*1,2,3-CICB^{1-}*	*1,2,3-CICB^{2-}*
r (C_1–C_2)	1.492	1.468	1.454
r (C_2–C_3)	1.492	1.468	1.456
r (C_3–C_4)	1.543	1.512	1.491
r (C_1–C_4)	1.530	1.503	1.482
r (C_4–O_7)	1.197	1.216	1.235
r (C_1–N_5)	1.279	1.301	1.324
r (N_5–C_{11})	1.332	1.326	1.315
r (C_{11}– N_{12})	1.171	1.174	1.182
α (C_2–C_1–N_5)	138.6	139.0	139.5
α (C_2–C_1–C_4)	90.5	90.4	90.6
α (C_1–C_4–C_3)	88.0	88.2	88.4
α (C_1–C_4–O_7)	136.6	136.2	135.9
α (C_1–N_5–C_{11})	122.7	123.2	125.6
α (N_5–C_{11}–N_{12})	172.3	171.0	169.8
d (N_5–C_1–C_4–O_7)	0.0	0.0	0.0
d (C_1–C_2–C_3–C_4)	0.0	0.0	0.0
d (C_2–C_1–N_5–C_{11})	0.0	0.0	0.0
d (C_1–N_5–C_{11}–N_{12})	180.0	180.0	180.0

* Bond lengths in Å, bond angles and dihedral angles in degrees.
† Optimized with the DFT method at B3LYP/6-31 + G(d,p) level in gas-phase.

The optimized geometries of **4**, **4a**, **4b** (equation (1)) in gas-phase are given in table 1 and figure 1. All the three geometries belong to Cs[$X(C_7N_6O)$] point group and each of them has a planar structure to allow the whole anion or neutral product to attain an energy minimum.

$$\underset{4}{1.2,3-\mathrm{CICB}^{2-}} \overset{E_1^0}{\rightleftharpoons} \underset{4a}{1.2,3-\mathrm{CICB}^{1-}} + \mathrm{e}$$
$$\underset{4a}{1.2,3-\mathrm{CICB}^{1-}} \overset{E_2^0}{\rightleftharpoons} \underset{4b}{1.2,3-\mathrm{CICB}^{0}} + \mathrm{e} \qquad (1)$$

In the dianion **4**, the distances (C_1–C_4), r(C_3–C_4) are 1.482 and 1.491 Å, respectively and may be considered equal (Wiberg bond index 1.03 and 1.04, respectively). r(C_1–C_2) and r(C_2–C_3) are shooter (1.454, 1.456 Å, Wiberg bond index 1.14), indicating a residual double bond character.

Among the three structures of group **4** (**4**, **4a** and **4b**), with the lost of one or two electrons compared with **4**, the r(C_1–C_2), r(C_2–C_3), r(C_3–C_4), r(C_1–C_4) and r(N_5–C_{11}) become longer and longer, but the r(C_4–O_7), r(C_1–N_5) and r(C_{11}–N_{12}) become shorter and shorter. These indicate that π-electron delocalization is weaker and weaker. Structures lacking of resultant negative charge, which is mainly located on the nitrogen atoms adjacent to the ring, have longer N–CN distances but shorter NCN–C (ring) bonds attributable to the greater electron affinity of the cyanoimino group compared to the rest of the molecular unit [19] (see section B).

Compared with group **4** (**4**, **4a** and **4b**), the corresponding r in each of the other four groups (**1**, **2**, **3**, **5** geometries belong to D_{4h}, C_s, C_{2v}, C_{4h}, respectively), has the same changes tendency (table 2). Compared the dianions among the five groups, with the number of NCN increase, r(C_1–N_5) and r(C_4–O_7) become shorter remarkably, but the bonds r(N_5–C_{11}) and r(C_{11}–N_{12}) change a little. The four bond distances of ring also averagely become shorter especially. In the dianions, r(C_1–N_5) is longer than r(N_5–C_{11}). These suggest that with the number of NCN increase, π-electron

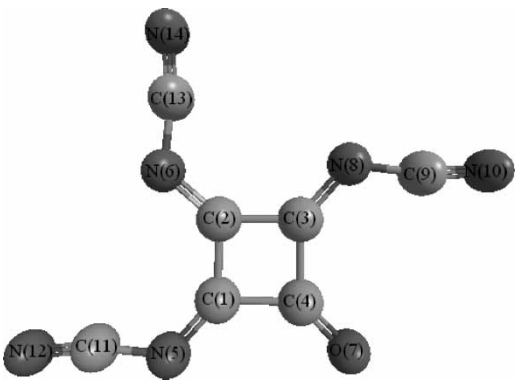

Figure 1. Optimized geometry of 1,2,3-CICB dianion.

Table 2. Optimized geometries of dianions (**1**, **2**, **3**, **4**, **5**) *†.

	1	*2*	*3*	*4*	*5*		
					Calc.	*Calc. Na_2(1,2,3,4-CICB)*	*X-ray [9] Na_2(1,2,3,4-CICB)*
r (C_1–C_2)	1.489	1.469	1.437	1.454	1.462	1.454	1.447
r (C_2–C_3)	1.489	1.505	1.483	1.456	1.462	1.454	1.447
r (C_3–C_4)	1.489	1.502	1.514	1.491	1.462	1.459	1.452
r (C_1–C_4)	1.489	1.462	1.483	1.482	1.462	1.459	1.452
r (C_4–O_7)	1.263	1.253	1.239	1.235			
r (C_1–N_5)		1.347	1.337	1.324	1.318	1.318	1.310
r (N_5–C_{11})		1.305	1.310	1.315	1.318	1.337	1.323
r (C_{11}– N_{12})		1.190	1.186	1.182	1.180	1.172	1.152

* Bond lengths in Å, bond angles and dihedral angles in degrees.
† Optimized with the DFT method at B3LYP/6-31 + G(d,p) level in gas-phase.

delocalization becomes stronger in the dianions from the atoms outside of the rings into those of the rings.

Compared the results of Na_2(1,2,3,4-CICB) (table 2), calculated at the same level as dianion **5**, with those of **5**, the $r(C_{11}–N_{12})$ in **5** is longer than that in Na_2(1,2,3,4-CICB), but the $r(C_5–N_{11})$ is shorter than that in Na_2(1,2,3,4-CICB), indicating that in **5**, without Na^+, the single or double bond character becomes unclear, suggesting that π-electron delocalization is quite strong in the dianion. It can also be seen in table 2 that the calculated bond lengths, angels and dihedral angels of Na_2(1,2,3,4-CICB) are very close to the corresponding experimental ones [9], suggesting that the DTF calculations are suitable for systems under investigation.

3.2 Charges

Natural charge populations (NPA) of group **4** (**4**, **4a** and **4b**) are listed in table 3 to analyze the distribution of electronic charge in the anions and neutral product. The most striking feature observed is that ΣC positive charge of the rings has nearly no change with the increase of the number of electron (1.109, 0.982 and 0.910 for **4b**, **4a**, **4**, respectively). But ΣNCN negative charge has greater change (−0.230, −0.486 and −0.751e for **4b**, **4a** and **4**, respectively). This suggests that resultant negative charge is mainly located on the atoms adjacent to the ring attributable to the greater electron affinity of the cyanoimino group compared to the rest of the unit. According to NPA, $\Sigma C_{SQ\ ring}$ charge of **4a** is contributed by α and β electron equally, but ΣNCN negative charge is contributed mainly by α electron, namely unpaired electron. The conclusions of this comparison agree with those drawn from ESR measurement [20].

Compared other four groups (**1**, **2**, **3** and **5**) with group **4**, they all have the resemble distribution trend of electronic charge in each group according to NPA. Comparing the derivatives holding the same net charge in different group, it is found that with the increase of number of NCN, the $\Sigma C_{SQ\ ring}$ negative charge increases and ΣNCN negative charge decreases at the same time (table 4), which indicate a rather spread out character for the π electrons. The symmetric 1,2,3,4-$CICB^{2-}$ dianion holds the largest spread among all the dianions.

3.3 NMR

The NMR shifts of these optimized geometries (SQ^{2-}, 1-$CICB^{2-}$, 1,2-$CICB^{2-}$, 1,2,3-$CICB^{2-}$ and 1,2,3,4-$CICB^{2-}$) are calculated at the GIAO-B3LYP/6-311++G(3df,3pd) level. Theoretical ^{13}C chemical shifts at the GIAO-RB3LYP/6-311++G(3df,3pd)//RB3LYP/6-31 + G(d,p) level listed in table 5 have been referenced to TMS $\delta(^{13}C) = 177.9 - \sigma(^{13}C)$.

For the B3LYP/6-31 + G(d,p) geometries of SQ^{2-}, 1-$CICB^{2-}$, 1,2-$CICB^{2-}$ and 1,2,3-$CICB^{2-}$ (figure 1) and

Table 3. NPA atomic charges of the anions of group **4***.

	*1,2,3-CICB (**4b**)*	*1,2,3-$CICB^{1-}$ (**4a**)*		*1,2,3-$CICB^{2-}$ (**4**)*
		α	β	
C_1	0.205	0.182	0.094	0.088	0.166
C_2	0.217	0.183	0.093	0.090	0.175
C_3	0.188	0.161	0.083	0.078	0.149
C_4	0.499	0.456	0.224	0.232	0.420
$\Sigma C_{SQ\ ring}$	**1.109**	**0.982**	**0.494**	**0.488**	**0.910**
O_7	−0.410	−0.525	−0.333	−0.192	−0.648
N_5	−0.375	−0.498	−0.348	−0.150	−0.626
C_{11}	0.400	0.421	0.239	0.182	0.444
N_{12}	−0.255	−0.409	−0.269	−0.140	−0.569
ΣNCN	**−0.23**	**−0.486**	**−0.378**	**−0.108**	**−0.751**

* Calculated with the DFT method at B3LYP/6-31G(d,p) level in gas-phase.

Table 4. NPA atomic charges of the anions of group **1**, **2**, **3**, **4**, **5***.

		C (neutral)	*B (monoanion)*			*A (dianion)*
				α	β	
1	$\Sigma C_{SQ\ ring}$	1.588	1.288	0.588	0.7	1.072
2	$\Sigma C_{SQ\ ring}$	1.423	1.193	0.558	0.635	1.044
	ΣNCN	−0.214	−0.534	−0.447	−0.087	−0.889
3	$\Sigma C_{SQ\ ring}$	1.262	1.092	0.528	0.564	0.986
	ΣNCN	−0.227	−0.514	−0.42	−0.094	−0.827
4	$\Sigma C_{SQ\ ring}$	1.109	0.982	0.494	0.488	0.911
	ΣNCN	−0.23	−0.486	−0.378	−0.108	−0.751
5	$\Sigma C_{SQ\ ring}$	0.956	0.864	0.452	0.412	0.824
	ΣNCN	−0.240	−0.466	−0.364	−0.102	−0.706

* Calculated with the DFT method at B3LYP/6-31G(d,p) level in gas-phase.

1,2,3,4-CICB^{2-}, the fit between the calculated and experimental [11] ^{13}C chemical shifts turn out to be consistently good. It is worth noting that the ^{13}C chemical shifts, in particular their large separation, are also reproduced quite well. Considering the fact that the calculation work is carried out on an unsolvated species and the experimentally obtained data are gathered from solution spectra, the obtained correspondence is excellent. Therefore, the GIAO-DFT results for all molecules suggest that the corresponding B3LYP/6-31 + G(d,p) geometries can be deemed reasonably good representations of the geometries of relatively free dianions in solution.

3.4 Oxidation potential

As reported in the literature [10], the dianions SQ^{2-} and *n*-CICB^{2-} (n_{sub} = 1, 2, 3, 4) can be oxidized reversibly in two consecutive steps to the corresponding radical monoanions and neutral forms (equation (1)). From the electrochemical data reported in table 6, it is evident that systematic substitution of the oxygen atoms in the $C_4O_4^{2-}$ structure with NCN groups causes a shift of both the oxidation potentials E_1^0 and E_2^0 towards more positive values, indicating that a consistent delocalization of the negative charge is exerted by these substituents. Electrochemical reactions can be achieved by a direct electron transfer at a certain potential. If electrons are transferred from the HOMO of a compound, a correlation is expected between the E_{HOMO} and the oxidation potential E_{ox}($E^0 = (E_p^a + E_p^c)/2$), because, the negatives of the orbital energies in the ground state are equal to the ionization potentials (I_p) according to Koopman's theorem. Kita *et al.* [21] correlated the limiting E_{ox} of five lithium tetraarylborates in 1,3-dioxolane/1,2-dimethoxyethane mixed solvents with their respective HOMO energies calculated using a semi-empirical molecular orbital method (MNDO). Barthel *et al.* [22] also proved this linear relationship using MNDO and AM1 for $B(O_2R)_2^-$ (R = C_6H_4, C_6H_3F, C_6H_4, $C_{10}H_6$)[22]. We correlate the limiting E_{ox}(E^0) of the 10 anions in five groups in dry, oxygen free acetonitrile (AN) with their respective HOMO energies calculated using HF and the I_p calculated using DFT molecular orbital methods.

3.4.1 *Ab initio* molecular orbital calculation. The limiting E_{ox} of the 10 anions in dry, oxygen free AN have been determined with the cyclic voltammograms (CV) of anions in the following two group order: **1** < **2** < **3** < **4** < **5**, **1a** < **2a** < **3a** < **4a** < **5a** (table 6). To examine this result, these HOMO energies are calculated using *ab initio* molecular orbital theory. The structures are optimized by HF/6-31 + G(d,p) and the energy calculations are further performed by HF/6-31++G(3df,3pd). The results are given in table 6 and figure 2, which shows a relatively good linear relationship between the HOMO energies and the limiting

Table 5. Experimental and calculated GIAO–RB3LYP/6-311++G(3df,3pd)//RB3LYP/6-31 + G(d,p) ^{13}C-NMR chemical shifts for **1**, **2**, **3**, **4**, **5**.

		C_{-O3}	C_{-O4}	C_{-N1}	C_{-N2}	C_{-N3}	$C_{-N3'}$
SQ^{-2}	Calc.	200.6					
	Exp.[9]	204.2					
1-CICB^{-2}	Calc.	202.9	201.3	196.0		127.5	
	Exp.[9]	201.0	196.5	192.0		123.9	
1,2-CICB^{-2}	Calc.	197.7		188.4		125.3	
	Exp.[9]	193.7		185.3		123.1	
1,2,3-CICB^{-2}	Calc.		186.7	186.0	177.5	120.7	121.2
	Exp.[9]		181.9	183.7	173.8	119.0	119.8
1,2,3,4-CICB^{-2}	Calc.			178.9		119.3	
	Exp.9			173.2		117.5	

Table 6. Limiting oxidation potentials, ionization potential calculations using DFT methods at 6-31++G(3df,3pd) level and HOMO energies using HF methods at 6-31++G(3df,3pd) level.

Anion	***1***	***1a***	***2***	***2a***	***3***	***3a***	***4***	***4a***	***5***	***5a***
$E_{radical}$ (a.u.)	−453.40415	−453.25788	−525.7865	−525.62652	−598.16483	−597.99347	−670.53716	−670.35716	−742.90698	−742.71971
E_{anion} (a.u.)	−453.33422	−453.40415	−525.74932	−525.7865	−598.15371	−598.16483	−670.54499	−670.53716	−742.93211	−742.90698
ΔE (KJ/mol)	−183.426	383.665	−97.52276	419.62589	−29.16765	449.47552	20.53801	472.13815	65.91573	491.20728
$ZPE_{radical}$ (KJ/mol)	89.331	90.176	116.112	116.671	143.976	144.642	172.202	173.304	200.131	201.351
ZPE_{anion} (KJ/mol)	89.811	89.339	117.715	116.112	145.531	143.976	173.613	172.202	201.655	200.131
ΔZPE (KJ/mol)	0.480	−0.837	1.603	−0.559	1.555	−0.666	1.411	−1.102	1.524	−1.220
I_p (KJ/mol)	**−183.906**	**384.502**	**−99.125**	**420.185**	**−30.723**	**450.142**	**19.127**	**473.240**	**64.392**	**492.427**
E_{HOMO} (KJ/mol)	**152.920**	**−460.571**	**59.830**	**−507.260**	**−13.246**	**−547.392**	**−62.112**	**−575.746**	**−105.995**	**−605.491**
E_{OX} [10] (mV vs. Pt)	**−120**	**810**	**167**	**1025**	**375**	**1204**	**544**	**1351**	**696**	**1470**

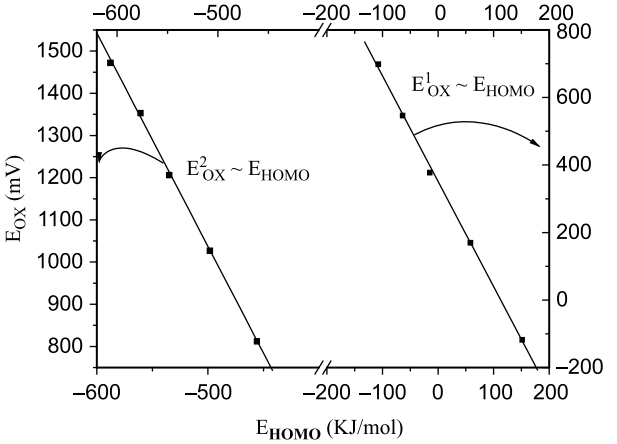

Figure 2. Relation between E_{ox} and E_{HOMO} of anions at HF/6-31++G(3df,3pd) level.

oxidation potentials. The regression results are:

$$E^1_{ox} = 352.01775 - 3.12413 * E_{HOMO} \quad (R = -0.99934)$$

(in gas-phase for **1**, **2**, **3**, **4**, **5**)

$$E^2_{ox} = -1305.34268 - 4.5937 * E_{HOMO} \quad (R = -0.99964)$$

(in gas-phase for **1a**, **2a**, **3a**, **4a**, **5a**).

3.4.2 DFT calculations. To further examine this experimental result, the I_p are calculated by DFT. This method usually gives higher accuracy in energy calculations, where the relative accuracies of various different model chemistries were considered by their performances on the *G*2 molecule sets [23]. The structural optimizations of the anions are carried out by B3LYP/6-31 + G(d,p) followed by the energy calculations on higher basis sets [24], 6-31++G(3df,3pd). Because Koopman's theorem is not valid in the DFT scheme, the adiabatic I_p is calculated from the energy difference ΔE between the total energy of the anion E_{anion} and that of the radical $E_{radical}$ or radical $E_{radical}$ and neutral $E_{neutral}$ generated by one-electron oxidation, as shown in equation (1). Zero-point energies (ZPE) are also calculated by frequency analysis using only B3LYP/6-31 + G(d,p). The ionization potentials are calculated from the following equation:

$$I_p = \Delta E - \Delta ZPE$$

The results are summarized in table 6 and figure 3. The I_p obtained by DFT methods are as a whole lower than those predicted from Koopman's theorem by *ab initio* MO methods. This is because Koopman's theorem neglects electron relaxation and electron correlation, which is important for the current systems containing anions. Figure 3 shows good correlation in two group between I_p and E_{ox}, completely confirming the experimental results: **1** < **2** < **3** < **4** < **5**, **1a** < **2a** < **3a** < **4a** < **5a**.

Table 7. Formation constant of the semiquinone form (monoanion).

	Dianion		ΔG_2° (298 K) (hartree)*	ΔG_1° (298 K) (hartree)†	ΔG_0° (298 K) (hartree)‡	$2(\Delta G_1^\circ (298\,K)) - \Delta G_2^\circ (298\,K) - \Delta G_0^\circ (298\,K)$ (kJ/mol)	$\log K_{sem}^{calc.}$	$\log K_{sem}^{exp.}$ [10]
2	1-CICB^{1-}	6-31 + G(d,p)	−525.695470	−525.732385	−525.570948	−520.27525	91.20	14.5
		SCRF(PCM) 6-31++G(3df,3pd)	−526.021334	−525.850949	−525.632442	−126.223511	22.13	
3	1,2-CICB^{1-}	6-31 + G(d,p)	−598.083605	−598.094774	−597.922234	−481.86682	84.47	14.1
		SCRF(PCM) 6-31++G(3df,3pd)	−598.400126	−598.222850	−598.000779	−117.496824	20.60	
4	1,2,3-CICB^{1-}	6-31 + G(d,p)	−670.460263	−670.452529	−670.271504	−454.54051	79.68	13.7
		SCRF(PCM) 6-31++G(3df,3pd)	−670.773319	−670.590212	−670.365358	−109.501951	19.19	
5	1,2,3,4-CICB^{1-}	6-31 + G(d,p)	−742.830346	−742.807582	−742.617950	−437.69305	76.72	13.1
		SCRF(PCM) 6-31++G(3df,3pd)	−743.145084	−742.956427	−742.730188	−98.577199	17.28	

* ΔG_2°(298 K), dianion Gibbs free energy.
† ΔG_1°(298 K), monoanion Gibbs free energy.
‡ ΔG_0°(298 K), neutral product Gibbs free energy.

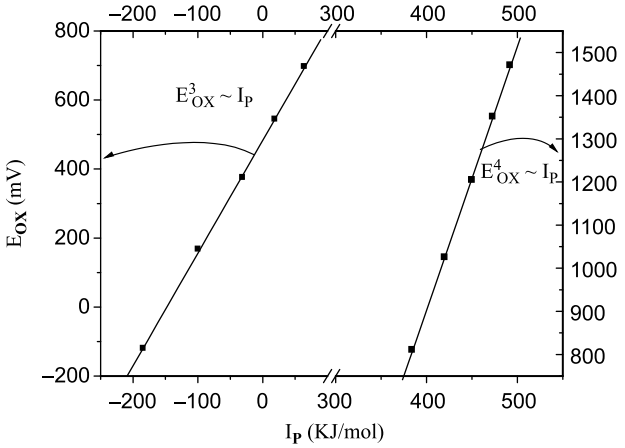

Figure 3. Relation between E_{ox} and I_p of anions at DFT B3LYP/6-31++G(3df,3pd) level.

The regression results are:

$$E^3_{ox} = 482.78946 + 3.26599{*}I_p \quad (R = -0.99984)$$
(in gas-phase for **1**, **2**, **3**, **4**, **5**)

$$E^4_{ox} = -1542.83071 + 6.11312{*}I_p \quad (R = 0.99993)$$
(in gas-phase for **1a**, **2a**, **3a**, **4a**, **5a**).

3.5 Formation constant of the semiquinone form (monoanion)

As reported in the literature, the dianions could be oxidized reversibly in two consecutive steps to the corresponding radical anions and neutral forms, equation (1). The experimental formation constants of the semiquinone (monoanion) form K_{SEM} were reported [10] (table 7). K_{SEM} is defined by the fraction, $[SEM]^2[RED]^{-1}[OX]^{-1}$ viz. $[monoanion]^2[dianion]^{-1}[natural]^{-1}$.

The calculated changes in the values of thermochemical functions ΔG^0 (298 K) and K_{sem} for chemical reaction (equation (2)) in gas-phase are reported in table 7.

$$n\text{-CDCB}^{2-} + n\text{-CDCB}^0 \rightarrow 2n\text{-CDCB}^{1-} \qquad (2)$$

These results are some distinct from the experimental findings. The linear relationship between calculated and experimental K_{sem} is relatively bad (figure 4). However, it should be said here that the experimental K_{sem} of the monoanions were measured in an AN solution of the anions and neutral products and so these distortions might be the result of interparticle interactions that occur in solution. In order to understand the effect of the interactions on the K_{sem} of the monoanions, we perform a SCRF (PCM) B3LYP/6-31++G(3df,3pd)//B3LYP/6-31 + G(d,p) study, as described before, using the anions and neutral products as solutes and AN as solvent. The results are reported in table 7. These results are excellent in agreement with the experimental findings. The linear relationship between calculated and experimental K_{sem} is relatively good (figure 4).

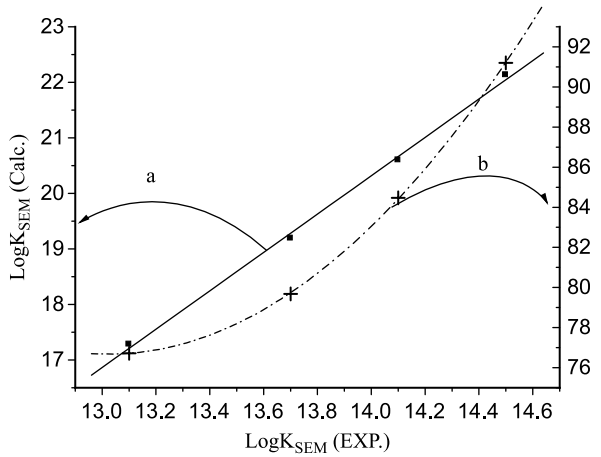

Figure 4. Relation between K_{sem}(calc.) and K_{sem}(exp.) of anions at DFT B3LYP/6-31++G(3df,3pd) level in AN solution (a) and in gas-phase (b).

The regression result is:

$$\log K_{sem}^{(calc.)} = -28.04075 + 3.45421 * \log K_{sem}^{(exp.)}$$
$$(R = 0.99904,\ \text{S.D.} = 0.11103)$$

These results suggest that the particles (anions and neutral products) should interact with solvents in solution and strongly suggest that in order to reproduce the experimental K_{sem} of the oxocarbons in solution, we must at least take into account the effect of the solvent.

4. Conclusion

We have presented a DFT study of the structures of anions of 1,2-dihydroxycyclo-buten-3,4-dione (squaric acid, H_2SQ) and the whole series of cyanoimino derivatives in gas-phase and in AN solution. Energetic calculations suggest that the most stable geometries of **1**, **2**, **3**, **4**, **5** are belonging to D_{4h}, C_s, C_{2v}, C_s and D_{2d}, respectively. NBO analyses indicate that with the number of NCN increase, π-electron delocalization become stronger in the dianion from the atoms outside of the ring into those of the ring. The GIAO-DFT results for all dianions suggest that the corresponding B3LYP/6-31 + G(d,p) geometries can be deemed reasonably good representations of the geometries of relatively free dianions in solution. The excellent correlations are also observed between experimental electrochemical stability E_{ox} and E_{HOMO}, or I_p, K_{sem} and Gibbs free energies calculated in AN solution.

Acknowledgements

This work was support by Chinese Academy of Sciences Hundred Talents program and the National Science Foundation of China (Grant No. 50372064).

References

[1] B. Gerecht, T. Kaempchen, K. Koeler, W. Massa, G. Offermann, R.E. Schmidt, G. Seitz, R. Sutrisno. Pseodooxokohlenstoff-dianionen der C_4-reihe mit dicyanmethylenfunktioneni. *Chem. Ber.*, **117**, 2714 (1984).
[2] A. Caneschi, D. Gatteschi, R. Sessoli. Toward molecular magnets: the metal–radical approach. *Acc. Chem. Res.*, **22**, 392 (1989).
[3] J.M. Williams, M.A. Beno, H.H. Wang, P.C.W. Leung, T.J. Emge, V. Geiser, K. Douglas Carlson. Organic superconductors: structural aspects and design of new materials. *Acc. Chem. Res.*, **18**, 261 (1985).
[4] M.R. Bryce, L.C. Murphy. Organic metals. *Nature*, **309**, 119 (1984).
[5] F. Wudl. From organic metals to superconductors: managing conduction electrons in organic solids. *Acc. Chem. Res.*, **17**, 227 (1984).
[6] J.B. Torrance. The difference between metallic and insulating salts of tetracyanoquinodimethone (TCNQ): how to design an organic metal. *Acc. Chem. Res.*, **12**, 79 (1979).
[7] R.C. Wheland, J.L. Gillson. Synthesis of electrically conductive organic solids. *J. Am. Chem. Soc.*, **98**, 3916 (1976).
[8] A.F. Garito, A.J. Heeeer. Design and synthesis of organic metals. *Acc. Chem. Res.*, **7**, 232 (1974).
[9] K. Koeler, W. Massa, G. Offermann, G. Seitz, R. Sutrisno. Iminocarbon dianions of the C_4-series with cyanoimino groups. *Chem. Ber.*, **118**, 1903 (1985).
[10] G. Seitz, P. Imming. Oxocarbons and pseudooxocarbons. *Chem. Rev.*, **92**, 1227 (1992).
[11] M. Ue, A. Murakami, S. Nakamura. Anodic stability of several anions examined by *ab initio* molecular orbital and density functional theories. *J. Electrochem. Soc.*, **149**(12), A1572 (2002).
[12] K. Tasaki. Computational study of salt association in Li-ion battery electrolyte. *J. Electrochem. Soc.*, **149**(4), A418 (2002).
[13] P. Johansson, S.P. Gejji, J. Tegenfeldta, J. Lindgren. The imide ion: potential energy surface and geometries. *Electrochim. Acta*, **43**(10-11), 1375 (1998).
[14] C. Lee, W.T. Yang, R.G. Parr. Development of the Colle–Salvetti correlation-energy formula into a functional of the electron density. *Phys. Rev. B*, **37**, 785 (1988).
[15] P.J. Hay, W.R. Wadt. *Ab initio* effective core potentials for molecular calculations. Potentials for the transition metal atoms Sc to Hg. *J. Chem. Phys.*, **82**, 270 (1985).
[16] Zh.M. Xue, Ch.H. Chen. Density functional theory study on lithium bis[1,2- benzenediolato(2-)-*O*,*O*′] borate and its derivatives: electronic structures, energies and molecular properties. *Electrochim. Acta.*, **49**, 5167 (2004).
[17] NBO version 3.1, E.D. Glendening, A.E. Reed, J.E. Carpenter, F. Weinhold.
[18] M.J. Frisch, G.W. Trucks, H.B. Schlegel, G.E. Scuseria, M.A. Robb, J.R. Cheeseman, J.A. Montgomery Jr., T. Vreven, K.N. Kudin, J.C. Burant, J.M. Millam, S.S. Iyenger, J. Tomasi, V. Barone, B. Mennucci, M. Cossi, G. Scalmani, N. Rega, G.A. Petersson, H. Nakatsuji, M. Hada, M. Ehara, K. Toyota, R. Fukuda, J. Hasegawa, M. Ishida, T. Nakajima, Y. Honda, O. Kitao, H. Nakai, M. Klene, X. Li, J.E. Knox, H.P. Hratchian, J.B. Cross, V. Bakken, C. Adamo, J. Jaramillo, R. Gomperts, R.E. Stratmann, O. Yazyev, A.J. Austin, R. Cammi, C. Pomelli, J.W. Ochterski, P.Y. Ayala, K. Morokuma, G.A. Voth, P. Salvador, J.J. Dannenberg, V.G. Zakrzewski, S. Dapprich, A.D. Daniels, M.C. Strain, O. Farkas, D.K. Malick, A.D. Rabuck, K. Raghavachari, J.B. Foresman, J.V. Ortiz, Q. Cui, A.G. Baboul, S. Clifford, J. Cioslowski, B.B. Stefanov, G. Liu, A. Liashenko, P. Piskorz, I. Komaromi, R.L. Martin, D.J. Fox, T. Keith, M.A. Al-Laham, C.Y. Peng, A. Nanayakkara, M. Challacombe, P.M.W. Gill, B. Johnson, W. Chen, M.W. Wong, C. Gonzalez, J.A. Pople. *Gaussian 03, Revision C.02*, Gaussian, Inc., Wallingford CT (2004).
[19] G. Famia, B. Lunelli, F. Marcuzzi, G. Sandoná. Dicyanomethylene derivatives of squaric acid: electrochemical behaviour and ESR investigation. *J. Electroanal. Chem.*, **404**, 261 (1996).
[20] V. Busetti, B. Lunelli. Characterization and crystal structure of the disodium salt of 1,2-carbodicyanocyclobuten-3,4-dione. *J. Phys. Chem.*, **90**, 2052 (1986).

[21] F. Kita, A. Kawakami, T. Sonoda, H. Kobayashi. In *New Sealed Rechargeable Batteries and Supercapacitors*, B.M. Barnett, E. Dowgiallo, G. Halpert, Y. Matsuda, Z.-I. Takehara (Eds.), p. 321, PV93-23, The Electrochemical Society Proceedings Series, Pennington, NJ (1993).
[22] J. Barthel, R. Buestrich, E. Carl, H.J. Gores. A new class of electrochemically and thermally stable lithium salts for lithium battery electrolytes III. Synthesis and properties of some lithium organoborates. *J. Electrochem. Soc.*, **143** (11), 3572 (1996).
[23] W.L. Jorgensen, J.M. Briggs. A priori pKa calculations and the hydration of organic anions. *J. Am. Chem. Soc.*, **111**, 4190 (1989).
[24] J. B. Foresman, A. Frisch. *Exploring Chemistry with Electronic Structure Methods*, 2nd ed., Gaussian, Pittsburgh PA (1996).